

# Particle-in-cell simulations for Nanoplasmonic Laser Induced Fusion Experiments

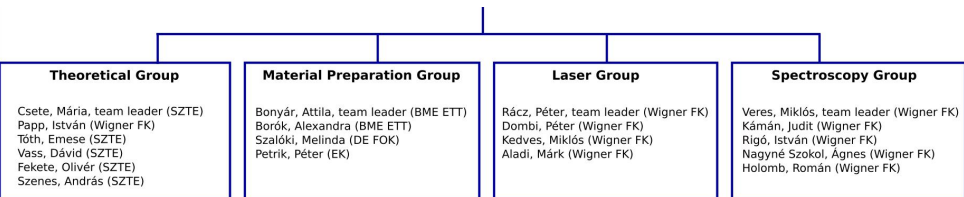
István Papp, Larissa Bravina, Mária Csete, Igor N. Mishustin, Dénes Molnár, Anton Motornenko, Leonid M. Satarov, Horst Stöcker, Daniel D. Strottman, András Szenes, Dávid Vass, Tamás S. Biró, László P. Csernai, Norbert Kroó



FIAS Frankfurt Institute  
for Advanced Studies



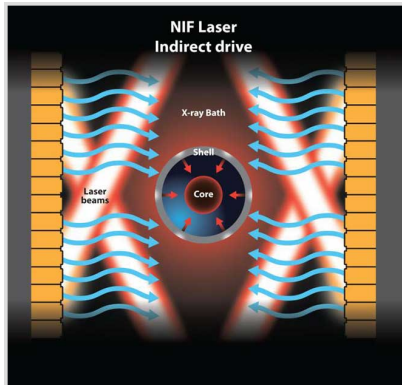
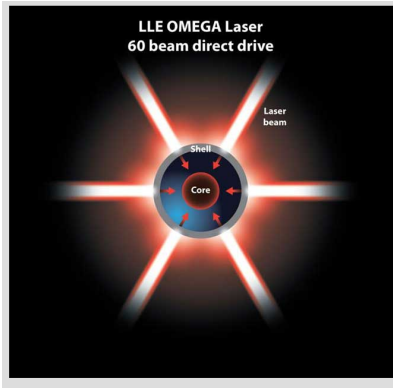
# Nanoplasmonic Laser Fusion Research Laboratory



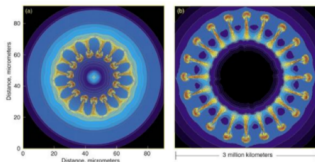
# Thermo-nuclear Fusion

- Fusion does not happen spontaneously on Earth
- Total fusion energy  $E_f = \frac{1}{4}n^2\tau\epsilon\langle v\sigma\rangle$
- $\eta E_f$  is the usable energy
- The loss is  $(1 - \eta)(E_0 + E_b)$
- $E_0 = 3nkT$ ,  $E_b = bn^2\tau\sqrt{T}$  (thermal bremsstrahlung)
- Giving the gain factor:  $Q = \frac{\eta\epsilon n\tau v\sigma}{4(1-\eta)(3kT+bn\tau\sqrt{T})}$
- $Q$  must be  $Q > 1$  for energy production
- This also means  $n\tau > \frac{3kT(1-\eta)}{\frac{1}{4}\epsilon\eta\langle v\sigma\rangle - b(1-\eta)\sqrt{T}} \rightarrow \text{LC}$
- Fulfilling the Lawson criterion
  - Magnetically confined plasmas: increase confinement time
  - Inertial confinement fusion: increase density of fusion plasma

# Direct vs Indirect drive



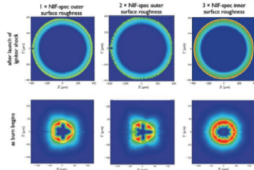
# Rayleigh-Taylor instabilities



Energy must be delivered as  
symmetric as possible!

Different levels of corrugation of the shell  
surfaces :

Striking similarities exist between hydrodynamic instabilities in (a) inertial confinement fusion capsule implosions and (b) core-collapse supernovae explosions. Image (a) is from Sakagami and Nishihara, *Physics of Fluids* #2, 2715 (1990); image (b) is from Hachisu et al., *Astrophysical Journal* 368, L27 (1991).



**Left:** same roughness of inner and outer surface as specified for the NIF target

**Center:** outer surface roughness is twice the NIF level

**Right:** DT inner surface roughness three times larger than NIF specifications

[S. Atzeni et al., *Nucl. Fusion* 54, 054008 (2014).]

25

# RFD

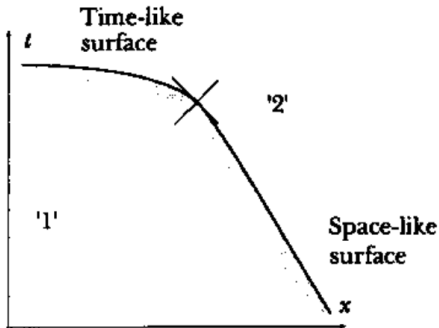
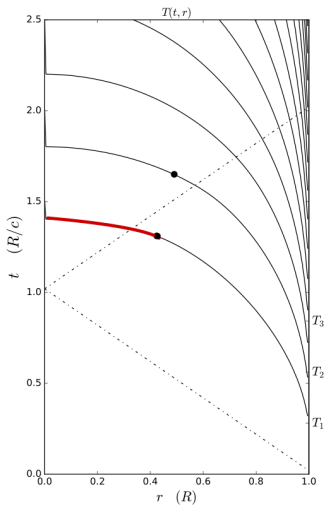


Figure 5.10: Smooth change from spacelike to timelike detonation  
[Csernai, L.P. (1987). Detonation on a time-like front for relativistic systems. Zh. Eksp. Teor. Fiz. 92, 379-386.]

# Constant absorptivity



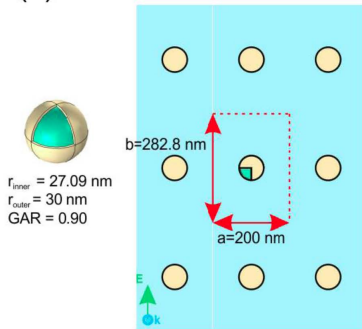
[L.P. Csernai & D.D. Strottman, *Laser and Particle Beams* 33, 279 (2015)]

$$\alpha_{k_{middle}} = \alpha_{k_{edge}}$$

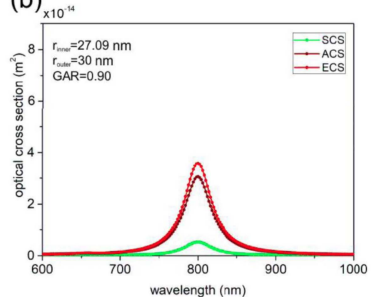
Simultaneous volume ignition is only up to 12%

# Doping with gold

(a)



(b)

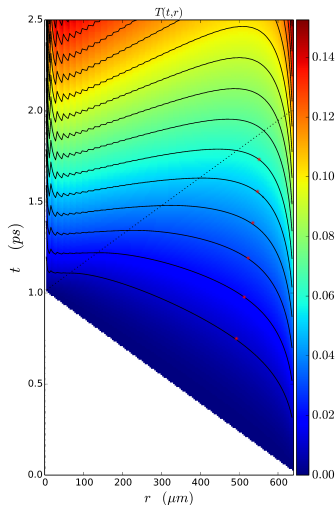


(a) Left: Single core-shell nano-sphere. Right: Rectangular lattice of nano-spheres in a transverse layer of the target.

(b) Optical cross-section of an individual core-shell nano-sphere optimized to absorb light at 800 nm wavelength and optical response of the same core-shell nano-spheres composing a rectangular lattice.



## Changing absorptivity

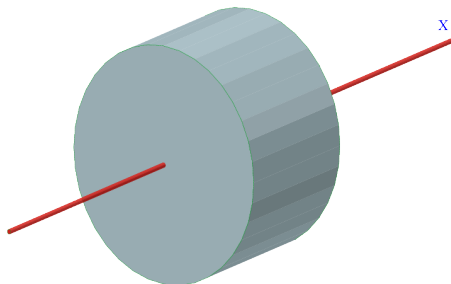


[Csernai, L.P., Kroo, N. and Papp, I. (2017). Procedure to improve the stability and efficiency of laser-fusion by nano-plasmonics method. Patent P1700278/3 of the Hungarian Intellectual Property Office.]

$$\alpha_{k_{middle}} \approx 4 \times \alpha_{k_{edge}}$$

Simultaneous volume ignition is up to 73%

# Flat target

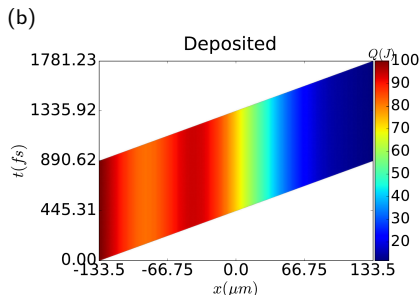
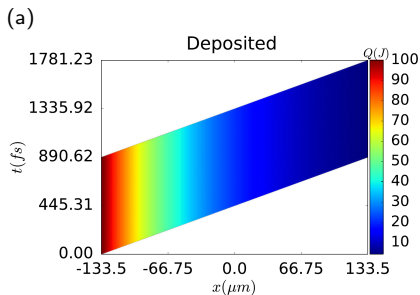


Schematic view of the cylindrical, flat target of radius,  $R$ , and thickness,  $h$ .

$$V = 2\pi R^3, \quad R = \sqrt[3]{V/(2\pi)}, \quad h = \sqrt[3]{4V/\pi}.$$

[L.P. Csernai, M. Csete, I.N. Mishustin, A. Motorenko, I. Papp, L.M. Satarov, H. Stcker & N. Kroó, Radiation- Dominated Implosion with Flat Target, *Physics and Wave Phenomena*, **28** (3) 187-199 (2020)]

# Varying absorptivity



**Deposited energy** per unit time in the space-time plane across the depth,  $h$ , of the flat target. **(a) without nano-shells (b) with nano-shells**

To increase central absorption we used the following distribution:

$$\alpha_{ns}(s) = \alpha_{ns}^C + \alpha_{ns}(0) \cdot \exp \left[ 4 \times \frac{\left(\frac{s}{100}\right)^2}{\left(\frac{s}{100} - 1\right) \left(\frac{s}{100} + 1\right)} \right].$$

# Particle In Cell methods

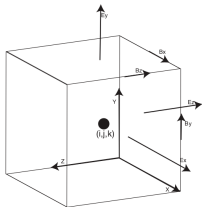


Figure 1. Yee staggered grid used for the Maxwell solver in EPOCH.

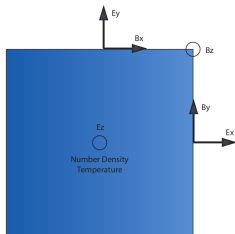


Figure 2: The Yee grid in 2D

[F.H. Harlow (1955). A Machine Calculation Method for Hydrodynamic Problems. Los Alamos Scientific Laboratory report LAMS-1956]

[T.D. Arber et al 2015 Plasma Phys. Control. Fusion 57 113001]

A **super-particle** (**marker-particle**) is a computational particle that represents many real particles.

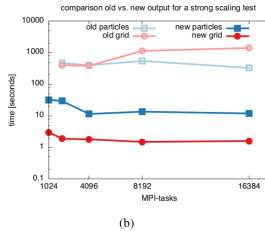
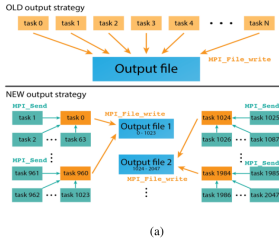
Particle **mover** or **pusher** algorithm as standard **Boris algorithm**.

**Finite-difference time-domain method** for solving the time evolution of **Maxwell's equations**.

# Available software

Computational application	Web site	License	Availability	Canonical Reference
SHARP	[17]	Proprietary		doi:10.3847/1538-4357/aa6d13
ALaDyn	[18]	GPLv3+	Open Repo:[19]	doi:10.5281/zenodo.49553
EPOCH	[20]	GPL	Open to academic users but signup required [21]	doi:10.1088/0741-3335/57/11/113001
FBPIC	[22]	3-Clause-BSD-LBNL	Open Repo:[23]	doi:10.1016/j.cpc.2016.02.007
LSP	[24]	Proprietary	Available from ATK	doi:10.1016/S0168-9002(01)00024-9
MAGIC	[25]	Proprietary	Available from ATK	doi:10.1016/0010-4655(95)00010-D
OSIRIS	[26]	Proprietary	Closed (Collaborators with MoU)	doi:10.1007/3-540-47789-6_36
PICCANTE	[27]	GPLv3+	Open Repo:[28]	doi:10.5281/zenodo.48703
PICLas	[29]	Proprietary	Available from Institute of Space Systems <sup>®</sup> and Institute of Aerodynamics and Gas Dynamics <sup>®</sup> at the University of Stuttgart	doi:10.1016/j.crme.2014.07.005
PIConGPU	[30]	GPLv3+	Open Repo:[31]	doi:10.1145/2503210.2504564
SMILEI	[32]	CeCILL-B	Open Repo:[33]	doi:10.1016/j.cpc.2017.09.024
iPIC3D	[34]	Apache License 2.0	Open Repo:[35]	doi:10.1016/j.matcom.2009.08.038
The Virtual Laser Plasma Library	[36]	Proprietary	Unknown	doi:10.1017/S0022377899007515
VizGrain	[37]	Proprietary	Commercially available from Esgee Technologies Inc.	
VPIC	[38]	3-Clause-BSD	Open Repo:[39]	doi:10.1063/1.2840133
VSim (Vorpal)	[40]	Proprietary	Available from Tech-X Corporation	doi:10.1016/j.jcp.2003.11.004
Warp	[41]	3-Clause-BSD-LBNL	Open Repo:[42]	doi:10.1063/1.860024
WarpX	[43]	3-Clause-BSD-LBNL	Open Repo:[44]	doi:10.1016/j.nima.2018.01.035
ZPIC	[45]	AGPLv3+	Open Repo:[46]	

# Piccante

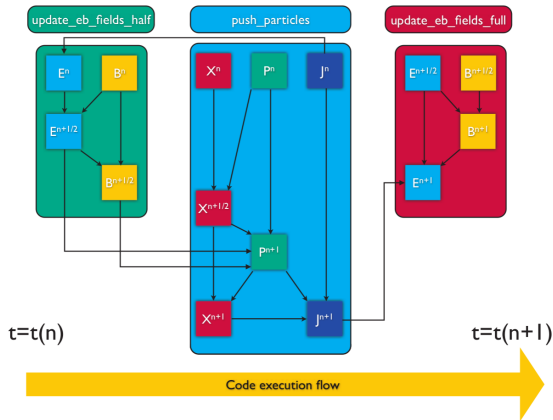


(a) Old and new strategies.  $G = 64$  group of tasks and  $F = N/128$  master tasks.

(b) Time spent for **writing particle positions** blue, time spent for **grid based outputs** (EM fields, densities) marked with red.

[A. Sgattoni, L. Fedeli, S. Sinigardi, A. Marocchino, A. Macchi, V. Weinberg, A. Karmakar; <https://arxiv.org/pdf/1503.02464.pdf>]

# General layout of the EPOCH code



[EPOCH 4.0 dev manual]

- (input) deck
- housekeeping
- io
- parser
- physics\_packages
- user\_interaction

## FDTD in EPOCH

- $\mathbf{E}_{n+\frac{1}{2}} = \mathbf{E}_n + \frac{\Delta t}{2} \left( c^2 \nabla \times \mathbf{B}_n - \frac{\mathbf{j}_n}{\epsilon_0} \right)$
- $\mathbf{B}_{n+\frac{1}{2}} = \mathbf{B}_n - \frac{\Delta t}{2} \left( \nabla \times \mathbf{E}_{n+\frac{1}{2}} \right)$
- Call particle pusher which calculates  $\mathbf{j}_{n+1}$
- $\mathbf{B}_{n+1} = \mathbf{B}_{n+\frac{1}{2}} - \frac{\Delta t}{2} \left( \nabla \times \mathbf{E}_{n+\frac{1}{2}} \right)$
- $\mathbf{E}_{n+1} = \mathbf{E}_{n+\frac{1}{2}} + \frac{\Delta t}{2} \left( c^2 \nabla \times \mathbf{B}_{n+1} - \frac{\mathbf{j}_{n+1}}{\epsilon_0} \right)$



# Particle pusher

- Solves the relativistic equation of motion under the Lorentz force for each marker-particle

$$\mathbf{p}_{n+1} = \mathbf{p}_n + q\Delta t \left[ \mathbf{E}_{n+\frac{1}{2}}(\mathbf{x}_{n+\frac{1}{2}}) + \mathbf{v}_{n+\frac{1}{2}} \times \mathbf{B}_{n+\frac{1}{2}}(\mathbf{x}_{n+\frac{1}{2}}) \right]$$

$\mathbf{p}$  is the particle momentum  $q$  is the particle's charge  $\mathbf{v}$  is the velocity.

$\mathbf{p} = \gamma m \mathbf{v}$ , where  $m$  is the rest mass  $\gamma = [(\mathbf{p}/mc)^2 + 1]^{1/2}$

- Villasenor and Buneman current deposition scheme [Villasenor J & Buneman O 1992 Comput. Phys. Commun. 69 306], always satisfied:  $\nabla \cdot \mathbf{E} = \rho/\epsilon_0$ , where  $\rho$  is the charge density.

## Particle shape

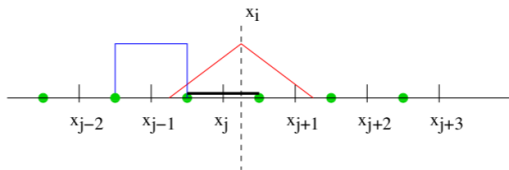


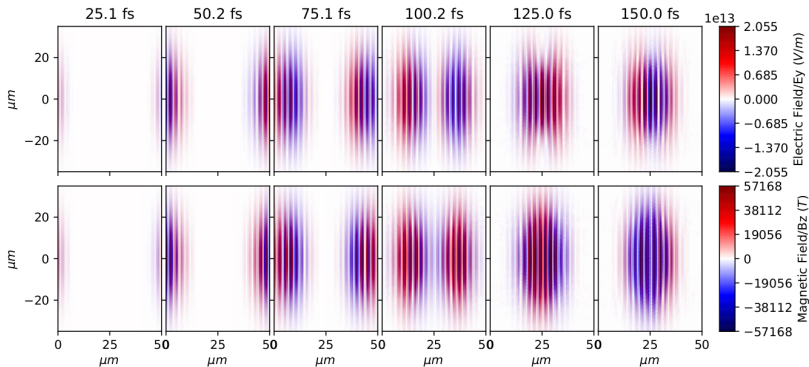
Figure 3: Second order particle shape function

First order approximations are considered

$$F_{part} = \frac{1}{2} F_{i-1} \left( \frac{1}{2} + \frac{x_i - X}{\Delta x} \right)^2 + \frac{1}{2} F_i \left( \frac{3}{4} - \frac{(x_i - X)^2}{\Delta x^2} \right)^2 + \frac{1}{2} F_{i+1} \left( \frac{1}{2} + \frac{x_i - X}{\Delta x} \right)^2$$

[EPOCH 4.0 dev manual]

# Colliding fields using EPOCH

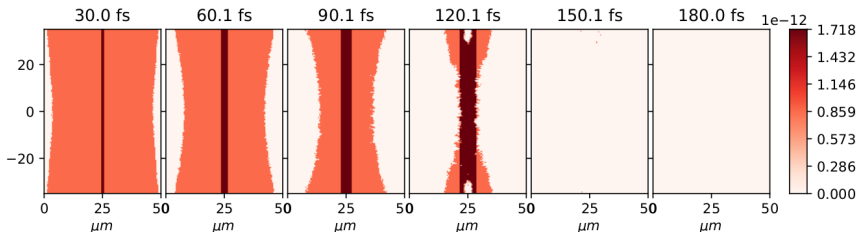


Laser parameters:

wavelength of  $\lambda = 1\mu\text{m}$ , full pulse length  $\Delta_t = 52\text{fs}$ , focus diameter is  $2R = 40\mu\text{m}$ ,  $3.0 \cdot 10^{19} \text{ W/cm}^2$  top intensity.

[Papp, I., et al., NAPLIFE Collaboration, Phys. Lett. A, (2021)]

## Multi-photon ionisation



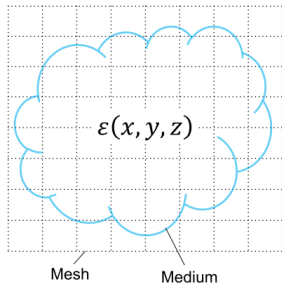
EPOCH includes a number of ionisation models by which electrons ionise in both the field of an intense laser and through collisions.

Epoch also includes Coulomb collisions

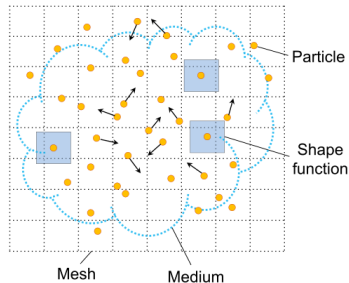
[K. Nanbu , S. Yonemura. Weighted particles in Coulomb collision simulations based on the theory of a cumulative scattering angle. *Journal of Computational Physics*, vol. **145**, pp. 639-654 (1998)]

# Nanorod

A Field simulation



B Particle simulation



[W. J. Ding, et al., Particle simulation of plasmons Nanophotonics, vol. 9, no. 10, pp. 3303-3313 (2020)]

# Nanorod

## Field solver:

$$\epsilon(\omega) = 1 - \frac{\omega_p^2}{(\omega^2 + i\gamma\omega)}$$

where  $\omega_p$  is the plasma frequency:  $\sqrt{\frac{n_e e^2}{m' \epsilon_0}}$

$\gamma$  is the damping factor or collision frequency:  $\gamma = \frac{1}{\tau}$  and  $\tau$  is the average time between collisions

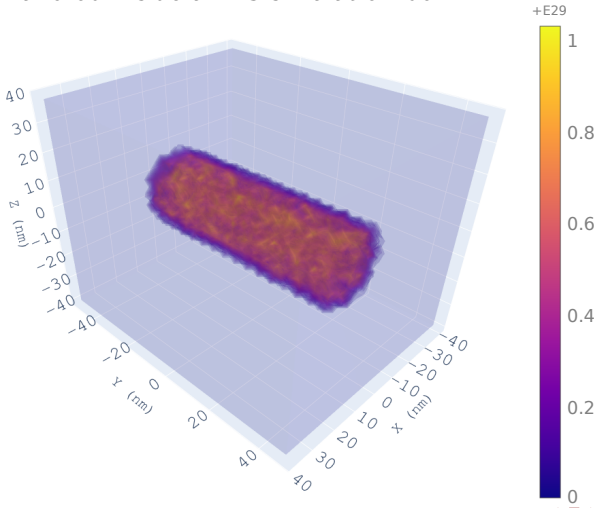
## Particle simulation:

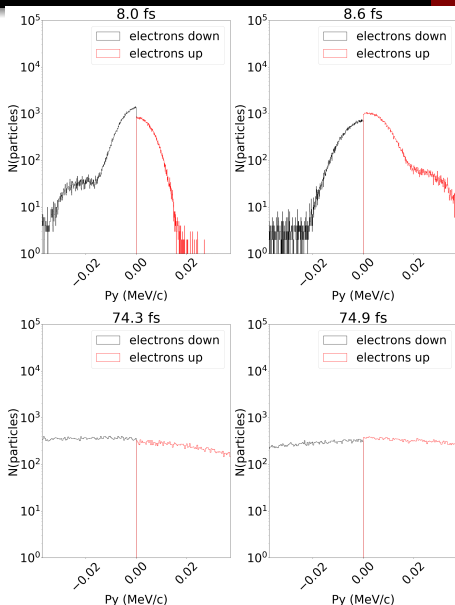
$$\frac{\partial \mathbf{E}}{\partial t} = \frac{1}{\mu_0 \epsilon_0} \nabla \times \mathbf{B} - \frac{\mathbf{J}}{\epsilon_0}, \quad \frac{\partial \mathbf{B}}{\partial t} = -\nabla \times \mathbf{E}$$

$\gamma_i m_i \mathbf{v}_i = q_i (\mathbf{E}_i + \mathbf{v}_i \times \mathbf{B}_i)$ ,  $\gamma_i$  is the relativistic factor

# Kinetic Modelling of the Nanorod

Nanorod inside a PIC simulation box





Considerations for the simulation box:

$$S_{CB} = 530 \times 530 \text{ nm}^2 =$$

$$2.81 \times 10^{-9} \text{ cm}^2 \text{ and length of}$$

$$L_{CB} = 795 \text{ nm}$$

beam crosses the box in

$$T = 795 \text{ nm} / c = 2.65 \text{ fs}$$

Nanorod size: 25 nm diameter  
 with 75 nm length

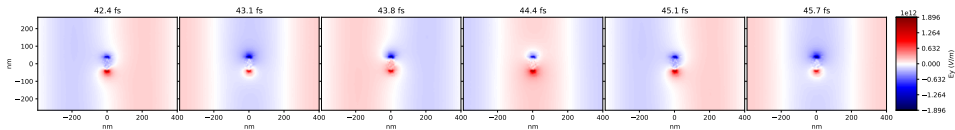
Pulse length:  $40 \times \lambda / c = 106 \text{ fs}$

Intensity:  $4 \times 10^{15} \text{ W/cm}^2$



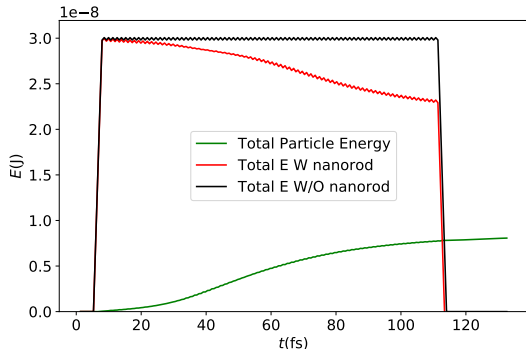
# Kinetic Modelling of the Nanorod

## Evolution of the fields



## $E_y$ evolution video

# Kinetic Modelling of the Nanorod



energy in the box **without nanorod** antenna  $3 \times 10^{-8}$  J (black line)

**nanorod** absorbs EM energy reducing it to  $2.3 \times 10^{-8}$  J (red line)

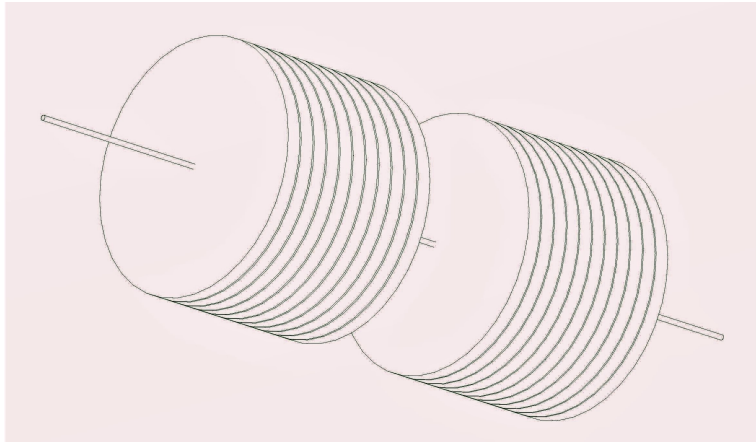
**deposited** energy in the nanorod (green line)

results in light absorption cross section nearly 35 times higher than its geometrical cross section

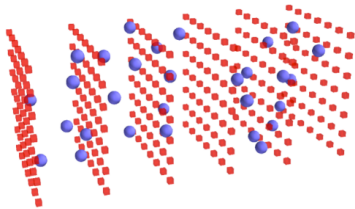
## Conclusions, Looking forward

- The model returns the analytical calculations regarding the absorption cross section
- The model is highly idealized
- Next step is material around the nanorods
- Fully dedicated software for the project is required
- Next step is estimating the target pre-compression

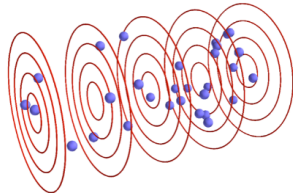
# Pre-compression



# Fourier-Bessel PIC method



**3D Cartesian grid**



**Cylindrical grid (schematic)**

[Rémi Lehe et al., A spectral, quasi-cylindrical and dispersion-free Particle-In-Cell algorithm, *Computer Physics Communications* Volume 203]